ORIGINAL ARTICLE-REGENERATION SCIENCE

Wound Repair and Regeneration — **WILEY**

Secretome of stem cells from human exfoliated deciduous teeth (SHED) and its extracellular vesicles improves keratinocytes migration, viability, and attenuation of H$_2$O$_2$-induced cytotoxicity

Juliana Girón Bastidas PhD [1,2] | Natasha Maurmann PhD [1,2] |
Juliete Nathali Scholl PhD [3] | Augusto Ferreira Weber MSc [3] |
Raíssa Padilha Silveira [1] | Fabricio Figueiró PhD [3,4] |
Marco Augusto Stimamiglio PhD [5] | Bruna Marcon PhD [5] | Alejandro Correa PhD [5] |
Patricia Pranke PhD [1,2,6]

[1]Hematology & Stem Cell Laboratory, Faculty of Pharmacy, Universidade Federal do Rio Grande do Sul, Porto Alegre, Rio Grande do Sul, Brazil

[2]Post Graduate Program in Biological Sciences: Physiology, Universidade Federal do Rio Grande do Sul, Porto Alegre, Rio Grande do Sul, Brazil

[3]Post Graduate Program in Biological Sciences: Biochemistry, Universidade Federal do Rio Grande do Sul, Porto Alegre, Rio Grande do Sul, Brazil

[4]Biochemistry Department, Universidade Federal do Rio Grande do Sul, Porto Alegre, Rio Grande do Sul, Brazil

[5]Stem Cells Basic Biology Laboratory, Instituto Carlos Chagas, FIOCRUZ/PR, Rua Professor Algacyr Munhoz Mader, Curitiba, Paraná, Brazil

[6]Stem Cell Research Institute (Instituto de Pesquisa com Células-tronco), Porto Alegre, Rio Grande do Sul, Brazil

Correspondence
Juliana Girón Bastidas, Hematology & Stem Cell Laboratory, Faculty of Pharmacy, Universidade Federal do Rio Grande do Sul, Ipiranga Av., 2752, room 304G. Zip code: 90610-000. Porto Alegre, Rio Grande do Sul, Brazil.
Email: jgironb@unal.edu.co

Abstract

Therapies for wound healing using the secretome and extracellular vesicles (EVs) of mesenchymal stem/stromal cells have been shown to be successful in preclinical studies. This study aimed to characterise the protein content of the secretome from stem cells from human exfoliated deciduous teeth (SHED) and analyse the in vitro effects of SHED-conditioned medium (SHED-CM) and SHED extracellular vesicles (SHED-EVs) on keratinocytes. EVs were isolated and characterised. The keratinocyte viability and migration of cells treated with SHED-EVs and conditioned medium (CM) were evaluated. An HaCaT apoptosis model induced by H$_2$O$_2$ in vitro was performed with H$_2$O$_2$ followed by 3-(4,5-dimethylthiazol-2-yl)-2,5-diphenyltetrazolium bromide (MTT) and live/dead assays. Finally, the expression of vascular endothelial growth factor (VEGF) in keratinocytes treated with secretome and EVs was evaluated by immunofluorescence staining and confirmed with RT-qPCR. SHED-EVs revealed a cup-shaped morphology with expression of the classical markers for exosomes CD9 and CD63, and a diameter of 181 ± 87 nm. The internalisation of EVs by HaCaT cells was confirmed by fluorescence microscopy. Proteomic analysis identified that SHED-CM is enriched with proteins related to stress response and development, including cytokines (CXCL8, IL-6, CSF1, CCL2) and growth factors (IGF2, MYDGF, PDGF). The results also indicated that 50% CM and 0.4–0.6 μg/mL EVs were similarly efficient for improving keratinocyte viability, migration, and attenuation of H$_2$O$_2$-induced

cytotoxicity. Additionally, expression of VEGF on keratinocytes increased when treated with SHED secretome and EVs. Furthermore, VEGF gene expression in keratinocytes increased significantly when treated with SHED secretome and EVs. Both SHED-CM and SHED-EVs may therefore be promising therapeutic tools for accelerating re-epithelialization in wound healing.

KEYWORDS
extracellular vesicles, keratinocytes, mesenchymal stem cells, mesenchymal stromal cells, secretome, tissue regeneration, wound healing

1 | INTRODUCTION

The study of mesenchymal stem/stromal cells (MSCs) has been an important focus of regenerative medicine. Over the years, many studies have employed these cells for systemic administration through intravenous/intravascular infusion or for direct application to injured sites, sometimes incorporating them into scaffolds. Their therapeutical properties were initially ascribed to their differentiation potential and/or their ability of homing to injury sites. However, it has been demonstrated that only a small proportion of transplanted MSCs can eventually survive and become integrated into the host tissue.[1] Furthermore, the systemic administration of MSCs carries a thrombogenic risk linked to tissue factor expression,[2] as well as a risk of embolisms related to the larger cell size of MSCs ($\approx$ 25 μm diameter, 465 ± 20 μm^2 surface area).[3]

Recently, the tissue regenerative properties of MSCs have also been associated with the release of bioactive factors with paracrine activity, including proteins and nucleic acids (microRNAs and messenger RNAs).[4] The secretome from MSCs has, therefore, created opportunities for studies focused on analysing the effects of MSCs conditioned medium and extracellular vesicles on injured tissue, thus avoiding the problems related to the direct use of the cells.

A variety of studies have demonstrated the efficacy of the secretome and EVs derived from different stem cell sources in wound healing.[5] MSCs secretome can therefore activate different signalling pathways involved in the skin regeneration process to enhance keratinocytes, fibroblasts, and endothelial cell activities.[5] In addition, these molecules can regulate ROS and cytokine levels and contribute to the macrophage transition into an anti-inflammatory profile M2.[5]

Stem cells from human exfoliated deciduous teeth (SHED) are self-renewing MSCs residing within the perivascular niche of the dental pulp.[6] These cells are a promising tool for regenerative medicine as they are a non-invasive source of highly accessible multipotent cells, with an excellent proliferation rate and no associated morbidity.[6,7]

Studies with SHED secretome and its EVs have shown significant recovery in various animal models of disease, including acute liver failure,[8] perinatal hypoxia-ischemia,[9] superior laryngeal nerve injury,[10] Parkinson's disease,[11] Alzheimer's disease,[12] experimental autoimmune encephalomyelitis,[13] diabetic polyneuropathy,[14] middle cerebral artery occlusion,[15] spinal cord injury model,[16] retinitis pigmentosa,[17] carrageenan-induced acute inflammation,[18] myocardial injury,[19] alopecia,[20] dental pulp regeneration,[21] calvarial defects,[22] periodontitis,[23] rheumatoid arthritis,[24] temporomandibular joint osteoarthritis,[25] glucose intolerance[26] and lung injury.[27] Recently, Xie and colleagues demonstrated in an LPS-induced wound healing model that SHED extracellular vesicles (SHED-EVs) could regulate macrophage function, stimulate macrophage autophagy, and subsequently induce an anti-inflammatory effect, thus contributing to wound healing.[28] However, the therapeutic potential of SHED secretome and its EVs on keratinocytes has not been examined.

In this study, we hypothesised that SHED secretome and EVs could contribute to accelerating re-epithelization. This study has therefore aimed to characterise the protein content from SHED secretome and to analyse the in vitro effects of SHED conditioned medium (SHED-CM) and SHED extracellular vesicles (SHED-EVs) on keratinocytes.

2 | MATERIALS

The products used from Sigma-Aldrich were 3-(4, 5-dimethylthiazol-2-yl)-2,5-diphenyl tetrazolium bromide (MTT), fluorescein diacetate (FDA), propidium iodide (PI), 4,6-diamidino-2-phenylindole (DAPI), PKH26 Red Fluorescent Cell Linker Mini Kit for General Cell Membrane Labelling, Dulbecco's Modified Eagle's Medium (DMEM/HEPES)-low glucose and high glucose, paraformaldehyde (PFA), trypsin–EDTA solution 10x Triton X-100 and bovine serum albumin (A9418). Fetal bovine serum (FBS) heat-inactivated from Cultilab, Campinas/SP, and dimethyl sulfoxide (DMSO) from Nuclear. The following antibodies were purchased from Invitrogen: VEGF Monoclonal Antibody (A183C 13G8), Catalogue # AHG0114, and Goat anti-Mouse IgG (H + L) Highly Cross-Adsorbed Secondary Antibody, Alexa Fluor 568 (A-11031). Bicinchoninic Acid Assay (BCA) (Thermo Scientific™, Catalogue #23225), Aldehyde/Sulphate Latex Beads, 4% w/v, 4 μm (Invitrogen, A37304), Purified Mouse Anti-Human CD9 (1:50, BD Bioscience, 555,370), Goat anti-Mouse IgG (H + L), Cross-Adsorbed Secondary Antibody, Alexa Fluor™ 488 (1:500, Invitrogen, A-11001) and Mouse Anti-Human CD63 (PE, 1:20, BD Bioscience, 556,020).

3 | METHODOLOGY

3.1 | Isolation and cultivation of SHED

SHEDs were obtained from 3 healthy donors, with the indication of tooth extraction. The teeth were sound, without a history of trauma or signs of clinical and radiographic pulp necrosis. The patients'

guardians signed a written consent approved by the Brazilian National Research Ethics Committee (Protocol number CAAE 12892419.0.0000.5347). The isolation, phenotype characterisation, and multipotency assay of SHED were performed as previously described.[29,30] The cells were cultivated in DMEM low glucose supplemented with 10% fetal bovine serum and 1% penicillin/streptomycin at 37°C under a 5% CO_2 atmosphere. Cells from passages 3–7 cells were used for all the experimental procedures.

3.2 | Preparation of conditioned media

For CM collection, 900,000 SHEDs were seeded in 182 cm^2 culture flacks and maintained in DMEM supplemented with 10% FBS and 1% penicillin/streptomycin until they reached 80% confluency. The cultures were then washed with phosphate-buffered saline (PBS) and cultivated for 48 h in FBS-free DMEM supplemented with 1% penicillin/streptomycin. The flacks selected to collect the CM were those with a low presence of dead cells visible under the microscope and with a culture medium without turbidity. The CM was filtered with a 0.2 μm pore membrane and stored at −35°C until use. The CM was collected between the third and seventh passages.

3.3 | Protein identification by LC-MS/MS and proteomic data analysis

For each sample, 20 μg of protein were mixed with 4× SDS-PAGE sample buffer (160 mM Tris-HCl pH 6.8, 4% SDS, 10% b-mercaptoethanol, 24% glycerol, and 0.02% bromophenol blue) to final buffer concentration of 1x and were resolved in 10% SDS-PAGE. The SDS-PAGE lanes were sliced and underwent gel trypsin digestion. The proteomics analysis was performed at the mass spectrometry facility RPT02H/Carlos Chagas Institute—Fiocruz Paraná. The peptides were analysed in duplicate by LC-MS/MS in an Ultimate 3000 RSLCnano online with an Orbitrap Fusion Lumos (Thermo Scientific Rochester, NY, USA). The chromatography was performed on a C18 in-house packed emitter with 15 cm length, 75 μm I.D., 3 μm particle (Dr. Maisch) with a flow of 250 nL/min and a linear gradient of 5%–40% acetonitrile in 0.1% formic acid for 120 min. The MS acquisition was done in DDA mode with MS1 spectra acquired in the orbitrap set to 120k resolution with automatic gain control standard, maximum injection time of 50 ms, and internal mass calibration enabled. Fragmentation was done using HCD, MS2 in the orbitrap set to 15k resolution with automatic gain control standard, and maximum injection time of 22 ms. The mass spectra obtained was analysed using the MaxQuant software (v. 2.0.3.0) set with default search parameters, MaxLFQ enabled, and using the Uniprot human protein database (79,052 entries).

The peptides identified only by site, reverse, and potential contaminants were removed. We considered as protein identified in a sample when having at least 1 unique peptide in at least two of the three biological replicates. The gene ontology analysis was performed using gProfiler, version e106_eg53_p16_65fcd97.[31]

3.4 | Extracellular vesicles isolation and characterisation

For EVs isolation, the CM was subjected to successive differential ultracentrifugation steps at 16,500 g for 63 min, followed by supernatant filtration with 0.2 μm membrane microfilter and double ultracentrifugation at 120,000 g for 70 min each. The EVs pellet was resuspended in PBS and the protein concentration was determined with a Bicinchoninic Acid Assay (BCA) kit.[32]

For EVs characterisation, the morphology was examined by transmission electron microscopy (TEM, Jeol JEM-1400 Plus, Tokyo) in Formvar-coated copper grids stained with uranyl acetate. The size distribution and concentration of the exosomes were analysed by nanoparticle tracking analysis (NTA) with NanoSight LM10 instrument (NanoSight Ltd, Amesbury, UK). To determine the expression levels of CD9 and CD63 in the EVs, the vesicles were coupled to beads and stained with specific antibodies for analysis by flow cytometry.[33] Briefly, beads (4 μm) able of binding to EVs were used. The EVs were stained with the primary antibodies CD9 (1:50) and CD63 (1:20) or a specific isotype control. Following this, the EVs were incubated with a secondary antibody specific to the primary antibody (Alexa Fluor™ 488,1:500). The EVs coupled to the beads were then washed twice and analysed using BD Accuri™ flow cytometer and C6 software (BD Biosciences, USA).

For the evaluation of the uptake of EVs by recipient cells, the EVs were labelled with PKH26. In accordance with the product instructions, 1 μL of PKH26 diluted in 250 μL of Diluent C was incubated with the isolated EVs at room temperature. After 5 min, 251 μL of FBS was added to halt the staining. The mixture was diluted with 1000 μL of PBS and centrifuged at 100,000 g at 4°C for 1 h. The pellet was washed with PBS and centrifuged again at 100,000 g. The labelled EVs were resuspended in DMEM and added to the HaCaT cells. After 17 h of incubation, the cells were washed with PBS and fixed with 4% paraformaldehyde for 20 min, rinsed in PBS and the cell nuclei were then blue stained with 0.5 μg ml^{-1} of DAPI (1 min). The photographs were obtained with the fluorescence microscope Leica DMi8 (Leica Microsystems).

3.5 | Keratinocytes viability

Immortalised epidermal HaCaT cells were cultivated in DMEM high glucose supplemented with 10% FBS and 1% penicillin/streptomycin) at 37°C under a 5% CO_2 atmosphere. For cell viability, the HaCaT cells were plated into 96-well plates (2000 cells/well). After 24 h, the HaCaT cells were treated with 50% CM from SHED and 50% FBS-free DMEM supplemented with 1% penicillin/streptomycin. Two days later, the cells were treated with 0.25 μg ml^{-1} of 3-(4,5-dimethylthiazol-2-yl)-2,5-diphenyltetrazolium bromide (MTT) for 2 h at 37°C. The supernatant was removed and 200 μL DMSO was added per well to dissolve the formed formazan crystals. Absorbance was measured at 560 and 630 nm with the equipment Multiskan™ FC Microplate Photometer (Thermo Scientific™).

The higher SHED-CM concentrations were then tested. The HaCaT cells were plated into 96-well plates (2000 cells/well). After

24 h, the HaCaT cells were treated with CM at 50%, 60%, 70%, 80%, 90%, or 100%. The culture medium was replaced on the third day and the MTT assay was carried out on the sixth day as described above.

To analyse SHED-EVs effects on HaCaT cell viability, the protein concentration of EVs isolated from 1 mL of complete CM was estimated by the following formula:

$$CMEVc = \frac{EVc \frac{\mu g}{\mu l} * PBS \, \mu l}{CM \, ml},$$

where 'CM EVc' is the protein concentration of extracellular vesicles in the SHED-CM. 'EVc' denotes the protein concentration of extracellular vesicles in the resuspended EVs pellet, 'PBS' stands for the volume of PBS used for EVs resuspension, and 'CM' signifies the volume of the conditioned medium used for EVs isolation.

Then, two EVs concentrations were chosen for the analysis: 0.4 and 0.6 μg/mL SHED-EVs. The control groups were cells treated with 0.4 and 0.6 μg/mL HaCaT-EVs and cells treated with FBS-free DMEM supplemented with 1% penicillin/streptomycin. The HaCaT cells were plated into 96-well plates (2000 cells/well) and treated after 24 h. The culture medium was replaced on the third day and the MTT assay was carried out on the sixth day as described above.

3.6 | Cell migration

The migratory properties of the HaCaT cells were analysed by the scratch test. The HaCaT cells were plated into 12-well plates at the density of 25×10^4 cells per well and cultivated for 24 h. Uniform scratch wounds were scraped by a sterile 200 μL pipette tip on the middle of the well. Each well was washed with PBS and then incubated with the corresponding test medium (50% SHED-CM, 0.4 μg/mL SHED-EVs, 0.4 μg/mL HaCaT-EVs, 50% HaCaT-CM, and DMEM). Microscopic images were taken immediately after scratch wounding and after 7 and 24 h with a Nikon Ti Eclipse microscope. The area of the wound gaps was measured using ImageJ software.

3.7 | HaCaT apoptosis model induced by H_2O_2

MTT assay was used to evaluate the survival of the HaCaT cells with different H_2O_2 treatments (550, 600, and 650 μM).

The HaCaT cells were then plated into 96-well plates at the density of 3×10^4 cells per well and cultivated for 48 h. The cultures were incubated with different H_2O_2 concentrations for 1 h, washed with PBS twice, and treated with DMEM, 50% SHED-CM, and 50% HaCaT-CM. The cells were maintained in standard culture conditions for 24 h. HaCaT viability was assessed by MTT assay. The live/dead assay was also used to confirm the results using an H_2O_2 600 μM concentration. A 10 μg/mL FDA and 5 μg/mL IP solution was then incubated with the cells for 20 min. The cells were washed with PBS and the photographs were obtained with the fluorescence microscope Leica DMi8 (Leica Microsystems).

3.8 | Immunofluorescence staining with vascular endothelial growth factor (VEGF)

HaCaT cells were plated into 96-well plates at the density of 3×10^4 cells per well and cultivated for 24 h. The cells were then treated with 50% SHED-CM, 0.4 μg/mL SHED-EVs, or FBS-free DMEM supplemented with 1% penicillin/streptomycin and cultivated for 24 h (4 wells per group). Subsequently, the cells were fixed in 4% paraformaldehyde (pH 7.4), permeabilized with 0.25% Triton X-100 and washed with PBS. The cells were incubated with a 1% BSA (PBS-BSA) solution for 1 h and then incubated overnight with primary antibody VEGF in PBS-BSA (1:200) at 4°C. The cells were washed twice with PBS and incubated with secondary antibody Goat anti-Mouse IgG, Alexa Fluor 568 (1:200) for 1 h at room temperature. The cells were washed (twice) and the photographs were obtained with the fluorescence microscope Leica DMi8 (Leica Microsystems). Images from four random fields per well were obtained and the mean fluorescence intensity in each field was calculated from grey values by ImageJ software.

3.9 | Real-time quantitative reverse transcription-polymerase chain reaction (RT-qPCR)

The HaCaT cells were seeded into 6-well plates at the density of 9.5×10^5 cells per well and cultivated for 24 h. The cells were then washed with PBS and treated with 1.8 mL of control (FBS-free DMEM supplemented with 1% penicillin/streptomycin), 50% SHED-CM or 0.4 μg/mL SHED-EVs and cultivated for 24 h (6 wells per group). The total mRNA of those cells was isolated using the TRIzol Reagent (Invitrogen, California, USA) according to the manufacturer's protocol. The quality and concentration of total RNA were examined using spectrophotometry and reverse transcription was performed with M-MLV Reverse Transcriptase (Promega Corporation, Wisconsin, USA), according to the manufacturer's instructions, with random primer as a template. Real-time PCR was performed in triplicate on a StepOnePlus™ Real-time PCR system (Applied Biosystems) using the GoTaq® qPCR Master Mix (Promega Corporation, Wisconsin, USA), also following the manufacturer's instructions, for the gene VEGFA (Forward:5′-ACGAAAGCGCAAGAAATCCC-3′, reverse: 5′-CTCCAGGG-CATTAGACAGCA-3′); VEGFR2 (Forward:5′- CAAGTGGCTAAGGG-CATGGA-3′, reverse: 5′-ATTTCAAAGGGAGGCGAGCA-3′ and gene expression was normalised to ACTB expression (Forward: 5′ CC-TGGCACCCAGCACAAT-3′, reverse: 5′-GACTCGTCATACTCCTGCTTG-3′). Relative quantification was calculated using the $2 - \Delta\Delta Ct$ method.[34]

3.10 | Statistical analysis

The results were expressed as the mean ± standard deviation. The one-way analysis of variance was applied, followed by post hoc Tukey or Duncan. The statistical programme used was PASW Statistics

18 software (SPSS Inc, Chicago, IL, USA) and the significance level used in the study was 5% ($p < 0.05$).

4 | RESULTS

4.1 | The secretome from SHED contains proteins related to stress response and development

To look into the secretome from SHED, first, a mass spectrometry analysis of the SHED-CM was performed. The analysis of the data identified 397 proteins (Supplementary Table 1), including proteins from extracellular space, EVs/exosomes, and cell-matrix (Table 1, Supplementary Tables 1 and 2). Gene ontology analysis showed that SHED-CM was enriched with proteins related to developmental

processes, such as anatomical structure development and morphogenesis, system and tissue development, developmental process, and multicellular organism development. Among them, we found matrix metalloproteinases (MMP2) and growth factors, such as insulin-like growth factor II (IGF2), myeloid-derived growth factor (MYDGF), and platelet-derived growth factor (PDGF). SHED-CM also contained proteins related to response to stimuli and stress, such as organonitrogen compound metabolic process, response to stress, cellular response to chemical stimulus, and to organic substance matrix. Among them, we found cytokines, such as interleukin-8 (CXCL8), interleukin-6 (IL-6), macrophage colony-stimulating factor 1 (CSF1) and C-C motif chemokine 2 (CCL2) (Table 1, Supplementary Tables 1 and 2), known as immunomodulatory (either pro- and anti-inflammatory), but also able to have protective and regenerative activities.[35]

TABLE 1 Gene ontology analysis of de 397 proteins found in SHED-CM.

	Term name	Adjusted _p_-value	Intersection size
GO:CC	Extracellular space	2.45E-194	323
	Extracellular vesicle	8.72E-185	274
	Extracellular membrane-bounded organelle	9.95E-185	274
	Extracellular organelle	9.95E-185	274
	Extracellular region	3.92E-183	340
	Extracellular exosome	6.28E-182	271
	Vesicle	8.80E-142	300
	Collagen-containing extracellular matrix	1.92E-58	82
	Extracellular matrix	3.29E-58	91
	External encapsulating structure	3.87E-58	91
	Secretory granule lumen	1.95E-54	71
	Cytoplasmic vesicle lumen	3.95E-54	71
	Vesicle lumen	6.28E-54	71
	Endoplasmic reticulum lumen	2.27E-50	67
	Secretory granule	3.44E-49	99
	Term name	**Adjusted _p_-value**	**Intersection size**
GO:BP	Anatomical structure development	1.64E-28	213
	Anatomical structure morphogenesis	1.05E-27	137
	Organonitrogen compound metabolic process	3.93E-27	225
	Response to stress	7.55E-26	164
	System development	1.02E-25	175
	Developmental process	6.30E-25	218
	Multicellular organism development	7.46E-25	184
	Cellular response to chemical stimulus	6.98E-24	139
	Response to chemical	7.08E-24	172
	Proteolysis	1.49E-23	103
	Response to stimulus	4.07E-23	264
	Response to organic substance	6.33E-23	137
	Tissue development	1.68E-22	106
	Cell adhesion	4.93E-22	91
	Extracellular matrix organisation	5.38E-21	43

Note: Top 15 terms with lower _p_-value for cell component (GO:CC) and biological process (GO:BP).

4.2 | Extracellular vesicles isolation and characterisation

Based on the results obtained by proteomic analysis, next was investigated in vitro the potential protective and pro-regenerative activity of the SHED-CM. As the proteomic analysis demonstrated the enrichment of proteins from EVs, it was also evaluated if EVs isolated from SHED could replicate the activity from the whole CM.

EVs from SHED were isolated by differential ultracentrifugation. TEM revealed a cup-shaped morphology for the EVs (Figure 1A). Moreover, the EVs expressed some of the classical markers described for exosomes (CD9 and CD63), which were detected by flow cytometry, as demonstrated in Figure 1B. NTA analyses showed high concentrations of vesicles with sizes ranging from 43 to 619 nm, Figure 1C. The mode particle size was found at 131.8 ± 9.5 nm and the EVs mean diameter was 180.5 ± 3.4 nm.

EVs internalisation by HaCaT cells was detected by labelling with the fluorescent dye PKH26. The PKH26-labelled EVs were incubated with HaCaT cells and after 17 h, the association of the red-labelled EVs with the blue nuclei of the HaCaT cells was observed by fluorescence microscopy. This assay demonstrated that the EVs were effectively internalised by the HaCaT cells (Figure 1D).

4.3 | Secretome from SHED and its EVs promotes HaCaT viability and migration

Secretomes from SHED and its EVs were tested to analyse their effect on HaCaT cell viability. Initially, the 50% SHED-CM group (containing 50% SHED-CM and 50% FBS-free DMEM supplemented with 1% penicillin/streptomycin) demonstrated a significantly increased viability when compared to the control (DMEM), Figure 2A. Greater concentrations of CM-SHED were then used to assess whether there
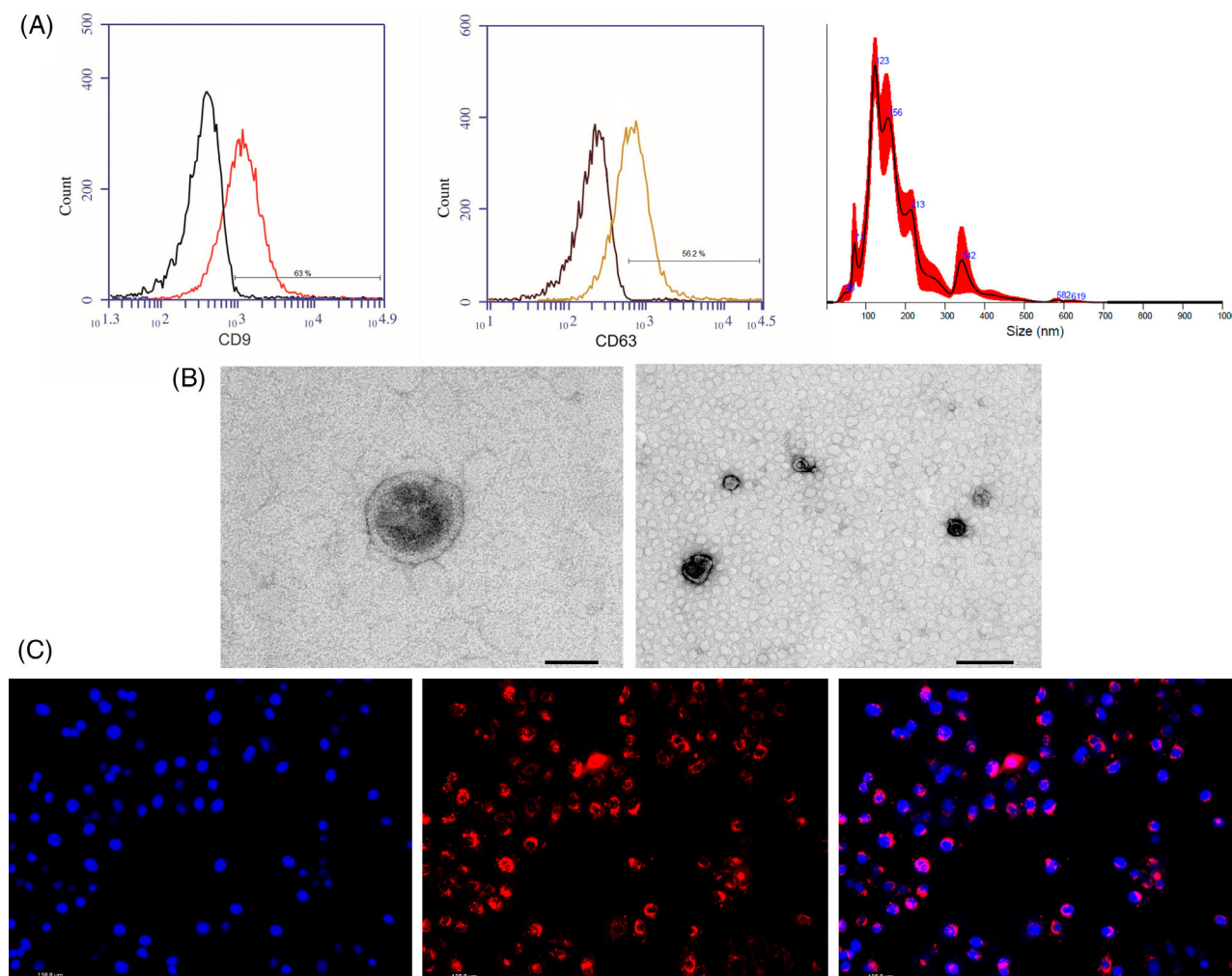
FIGURE 1 Characterisation of extracellular vesicles isolated from SHED. (A) Morphologic analysis of EVs by transmission electron microscopy (scale bar = 50 nm and 200 nm respectively). (B) Flow cytometry analysis of exosomal proteins CD9 (red) and CD63 (yellow) of EVs. Black: control. (C) The particle size of EVs was analysed by nanoparticle tracking analysis. (D) EVs uptake assay. EVs (stained in red by PKH26) were effectively internalised by the HaCaT cells (nuclei stained in blue by DAPI).
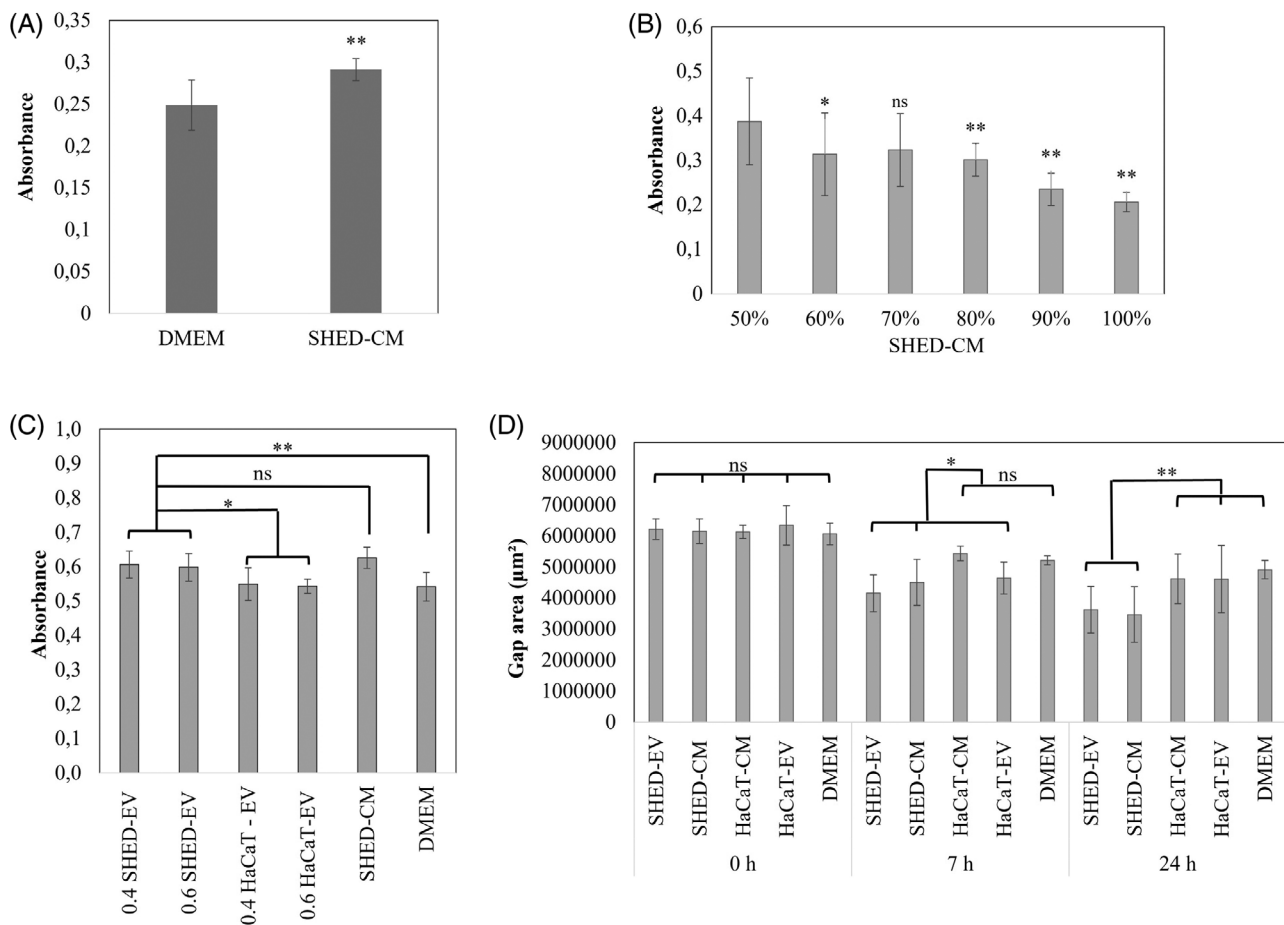
FIGURE 2 Viability (MTT reduction) and migration of HaCaT after treatment with stem cell secretome and its EVs. (A) MTT after treatment with 50% conditioned media (CM) for 2 days, $n = 10$. (B) MTT after use of 50%–100% conditioned media for 2 days $n = 16$. (C) MTT after use of 0.4 or 0.6 μg/mL of extracellular vesicles (EV) from SHED or HaCaT or 50% conditioned media (CM) of SHED for 2 days, $n = 8$. (D) Quantification of scratch closure (gap area) using the ImageJ after 0, 7, and 24 h of treatment with 50% SHED-CM, 0.4 μg/mL SHED-EVs, 0.4 μg/mL HaCaT-EVs, 50% HaCaT-CM and DMEM, $n = 3$. Data expressed as the mean ± SD. *$p \leq 0.05$ and **$p \leq 0.01$ indicate significance between groups and 'ns' no significance by one-way ANOVA followed by Tukey HSD post hoc test.

was a proportional relation between CM-SHED concentration and cell viability, Figure 2B. However, the MTT assay demonstrated an inversely proportional relation, showing less viability with concentrations greater than 50%.

Additionally, the protein concentration of EVs in complete CM was 0.77 ± 0.13 μg/mL, then, the EVs protein concentration at 50% CM was estimated as being approximately 0.4 μg/mL. Different concentrations from the isolated SHED-EVs were tested to evaluate HaCaT cell viability, Figure 2C. The results showed that SHED-EVs concentrations from 0.4 and 0.6 μg/mL were as effective as using 50% SHED-CM. In addition, the viability of both SHED-EVs concentrations was significantly increased when compared with similar concentrations from HaCaT-EVs and DMEM (control groups).

HaCaT cell migration was assessed by scratch assay (Figure 2D, Figure 3, and Table 2). For this assay, HaCaT-EVs, HaCaT-CM, and DMEM were used as controls. The results showed that cells in the presence of SHED-CM, SHED-EVs, and HaCaT-EVs presented a significant reduction in the gap area after 7 h when compared with the

control and HaCaT-CM at 7 h (Table 2). A total of 24 h later, the groups treated with SHED-CM and SHED-EVs presented a significant reduction in the gap area when compared with the HaCaT-EVs, HaCaT-CM, and DMEM treated groups. There was no difference between the SHED-CM and SHED-EVs treated groups. Results from the gap closure percentage presented in Table 2 showed a similar tendency of gap area results.

4.4 | Secretome from SHED and its EVs increase vascular endothelial growth factor (VEGF) expression in keratinocytes

VEGF mean fluorescence intensity was calculated on treated HaCaT cells. The results showed an increase in VEGF expression on HaCaT cells treated with SHED-CM and SHED-EVs when compared to the FBS-free DMEM group, Figure 4. No difference was seen between the SHED-CM and SHED-EV groups. Corroborating previous
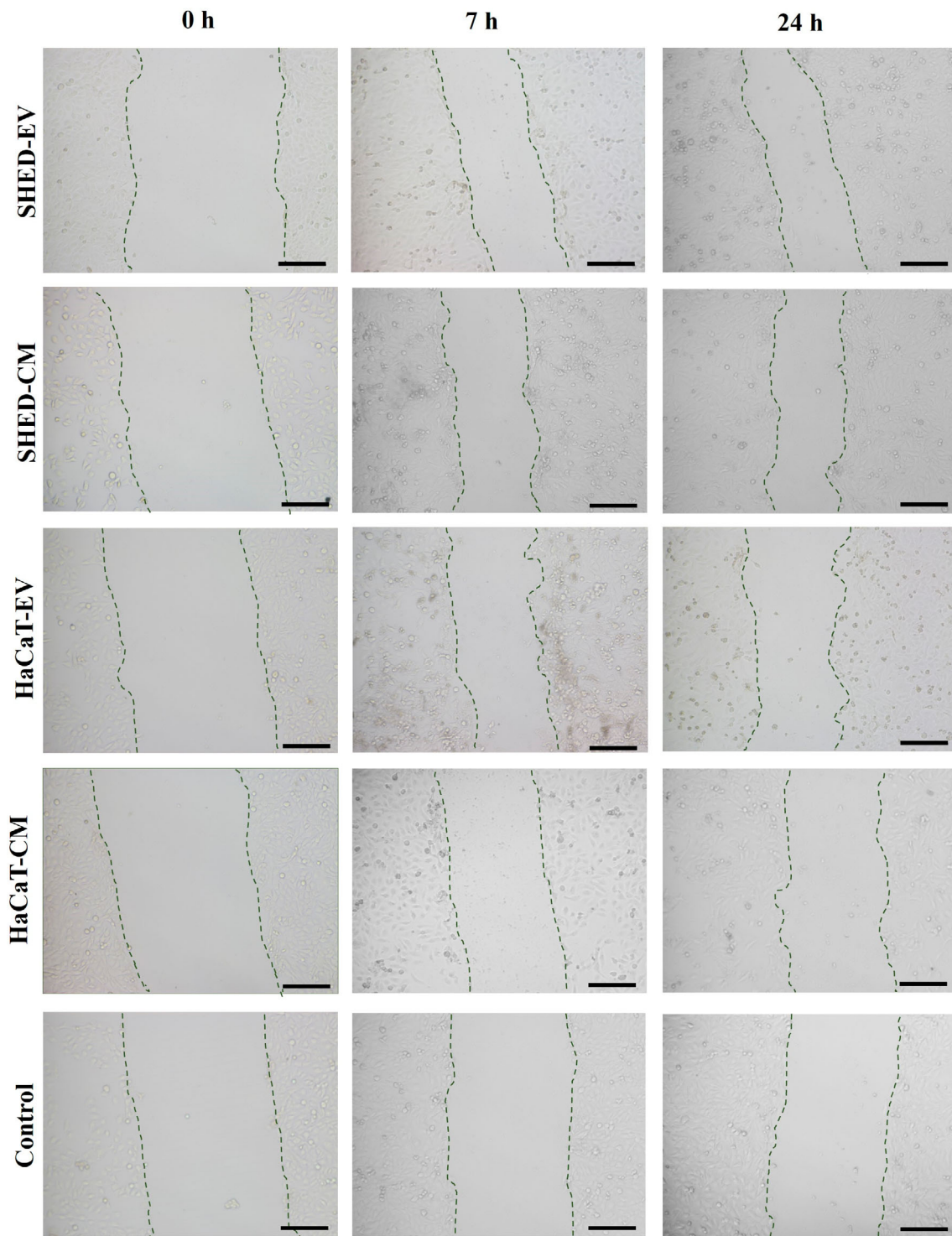
FIGURE 3 Scratch-wound assay of HaCaT cells after 0, 7, and 24 h of treatment with stem cell secretome and its EVs ($n = 3$). DMEM, HaCaT-CM and HaCaT-EV were used as controls. CM indicates conditioned media and EVs indicates extracellular vesicles. Scale bar = 200 μm.

findings, a substantial increase in VEGF-α gene expression levels was observed, with approximately a four-fold increase in cells treated with SHED-CM and a two-fold increase in cells treated with SHED-EV, compared to untreated cells (Figure 4D). Additionally, a significant upregulation of the VEGF receptor (VEGFR2) was detected in HaCaT cells following treatment with the SHED-CM (Figure 4D).

4.5 | Secretome from SHED and its EVs attenuate the suppression of cell viability induced by H_2O_2

HaCaT cell viability was assessed after treating the cells with different H_2O_2 concentrations to generate a skin cell damage model. As shown in Figure 5A, the cell viability of the HaCaT cells was significantly

TABLE 2 Scratch-wound assay results using the wound healing measurement tool of ImageJ of HaCaT treated with extracellular vesicles (EV) or conditioned media (CM) of SHED or HaCaT.

		SHED-EVs	SHED-CM	HaCaT-CM	HaCaT-EVs	DMEM
Gap area (µm²)	0 h	6,219,274 ± 331247 [a]	6,156,178 ± 395,099 [a]	6,130,652 ± 209,418 [a]	6,339,654 ± 633,132 [a]	6,064,759 ± 346,819 [a]
	7 h	4,156,217 ± 595,310 [a]	4,503,682 ± 742,185 [a]	5,435,375 ± 233306.8 [b]	4,641,254 ± 518,458 [a]	5,209,743 ± 144,406 [b]
	24 h	3,625,962 ± 749,496 [a]	3,465,290 ± 895,899 [a]	4,616,937 ± 797,973 [b]	4,613,819 ± 1081648.9 [b]	4,912,639 ± 294,649 [b]
Gap closure %	7 h	33.2 ± 9.6 [a]	26.8 ± 12.1 [a,b]	11.3 ± 3.8 [c]	26.8 ± 8.2 [a,b]	17.8 ± 2.3 [b]
	24 h	41.7 ± 12.1 [a,b]	43.7 ± 14.6 [a]	24.7 ± 13.0 [c]	27.2 ± 17.1 [b,c]	19.0 ± 5.3 [c]

Note: Data expressed as the mean ± SD. Different letters indicate significant differences among means ($p \leq 0.05$) and the same letters indicate statistical equivalence ('a', 'b' means statistical equivalence with both 'a' and 'b') as determined by one-way ANOVA followed by Duncan's post hoc test in each line (correspondent each experimental time of 0, 7, or 24 h).

inhibited by the application of H_2O_2 in a dose-dependent manner. The groups treated with 600 and 650 µM H_2O_2 (DMEM/600 µM and DMEM/650 µM), thereby presented a significant difference when compared to the DMEM control group. Additionally, when the cells were exposed to H_2O_2 600 µM and treated with SHED-CM, cell viability was not suppressed and presented no significant difference with the DMEM group. When the cells were exposed to H_2O_2 650 µM, the treatment with SHED-CM was not sufficient to attenuate cell viability suppression. The groups SHED-CM/650 µM, HaCaT-CM/550 µM, HaCaT-CM/600 µM, and HaCaT-CM/650 µM presented significantly reduced cell viability when compared to the DMEM group. No significant difference between these groups was observed.

Furthermore, to visually confirm the MTT assay results, a live/dead assay was performed, Figure 5B–G. The test was conducted using only H_2O_2 600 µM because SHED-CM treatment performed better with this concentration. Figure 5F shows a greater number of dead cells in the DMEM/600 µM group, while a greater number of live cells in the SHED-CM/600 µM and SHED-EVs/600 µM groups were observed (Figure 5B, C, respectively). In addition, the HaCaT-CM/600 µM and HaCaT-EVs/600 µM groups showed a greater number of live cells (Figure 5D, E, respectively), but with lower density when compared to the SHED-CM/600 µM and SHED-EVs/600 µM groups (Figure 5B, C, respectively).

5 | DISCUSSION

Epithelialization is an essential component of wound healing and a failure in this process may contribute to wound reoccurrence.[36] Therefore, complete epithelialization can be used as a defining parameter of wound healing success. In the case of partial-thickness wounds, re-epithelialization occurs primarily from stem/progenitor cells in the eccrine sweat glands and pilosebaceous units, and to a lesser extent from basal stem and progenitors in the interfollicular epidermis.[37] On the other hand, in full-thickness wounds, re-epithelialization occurs slower because keratinocytes originate from interfollicular epidermal cells at wound margins,[37] to later migrate to the centre of the wound.[38] In this context, analysing the effect of the secretome from SHED and its EVs on keratinocyte viability, migration, and attenuation of H_2O_2-induced cytotoxicity could be an interesting alternative for wound treatment.

In this study, the SHED-CM and SHED-EVs effects on keratinocytes (HaCaT cell line) were analysed for the first time. SHED-EVs were successfully characterised with the typical EVs markers CD9 and CD63, NTA, TEM, and PKH26 labelling.

The viability of keratinocytes was markedly increased with 50% SHED-CM, and greater concentrations were not effective, probably due to the absence of essential nutrients found in fresh media. It was also established that 0.4 and 0.6 µg/mL SHED-EVs were equally effective in enhancing keratinocyte viability as SHED-CM. These concentrations were selected based on the protein concentration of EVs isolated from the complete conditioned medium, which was measured

FIGURE 4 VEGF expression in keratinocytes. (A) DAPI stain. (B) VEGF immunofluorescence staining. (C) VEGF Fluorescence Intensity ($n = 4$). Data expressed as the mean ± SD. **$p \leq 0.01$ indicates significance between groups and 'ns' indicates no significance by one-way ANOVA followed by Tukey HSD post hoc test. Control: secondary antibody only. (D) Relative gene expression of VEGFA and VEGFR2 in keratinocytes treated with SHED-CM and SHED-EVs. VEGFA, vascular endothelial growth factor A; VEGFR2, vascular endothelial growth factor receptor 2. The data are presented as means from technical triplicate (mean ± SD). One-way ANOVA analyses were applied with Tukey's multiple comparisons test. Statistical significance: **$p<0.01$ versus DMEM, ****$p<0.0001$ versus DMEM, ####$p<0.0001$ versus SHED-CM.

at $0.77 \pm 0.13\,\mu g/mL$. This means that working with 50% CM is equivalent to working with approximately $0.4\,\mu g/mL$ of EVs, thus explaining the lack of difference between the EVs group and 50% CM. Additionally, keratinocyte migration was also improved when treated with SHED-CM and $0.4\,\mu g/mL$ SHED-EVs, outperforming the HaCaT-CM and $0.4\,\mu g/mL$ HaCaT-EVs controls. This enhancement in keratinocytes migration can be attributed to the presence of cell adhesion proteins, IL-6 and CXCL8 in SHED-CM (Table 1). Also, IL-6 and CXCL8 play crucial roles in the repair process and have been related to keratinocyte migration, differentiation, and proliferation.[39–43]

It is known that keratinocytes can express increased amounts of vascular endothelial growth factor during wound healing,[44] in addition, to expressing the three VEGF receptors (VEGFR-1, VEGFR-2, and VEGFR-3).[45,46] VEGF is widely recognised as an angiogenesis promoter; however, its healing functions could also be directed to non-endothelial cell types, such as keratinocytes. Wilgus and collaborators demonstrated that VEGF can stimulate keratinocyte proliferation in vitro and that the VEGFR-1 neutralisation leads to delayed re-epithelialization in vivo.[46] Additionally, it had previously been proven

that SHED-CM is rich in VEGF growth factor.[21,47] In the presented study, although our proteomic characterisation did not identify VEGF in SHED-CM, it was found that SHED-CM and SHED-EVs can markedly increase the VEGF expression on HaCaT cells. This increase was confirmed through immunofluorescence and RT-qPCR analyses. Thus, one plausible mechanism underlying the stimulation of keratinocyte proliferation and migration by the SHED secretome and EVs appears to involve the VEGF signalling pathway. Previous works have demonstrated that the conditioned medium from SHED contains other growth factors such as angiopoietin-2, epidermal growth factor (EGF), hepatocyte growth factor, stem cell factor, and transforming growth factor-α,[47] but also the anti-inflammatory cytokines TGF-β1 and IL-10, and proliferative cytokines IL-6 and IL-3, among others. Here, we also identified the cytokines CXCL8 (IL-8), IL-6, CSF-1, CCL2 (MCP-1) and growth factors such as PDGF, IGF2, IGFBPs,[2,4–7] MYDGF. Therefore, other possible signalling pathways should be explored.[47,48]

Finally, an HaCaT apoptosis model induced by H_2O_2 was established by exposing HaCaT cells to varying H_2O_2 concentrations. Treatment with $600\,\mu M$ H_2O_2 proved to be the most suitable, significantly

FIGURE 5 Skin lesion model. (A) MTT assay of HaCaT cells submitted to different H_2O_2 concentrations and then treated with DMEM (control), 50% conditioned media of HaCaT (HaCaT-CM, used as control) or 50% conditioned media of SHED (SHED-CM). Data expressed as the mean ± SD. *$p \leq 0.05$ indicates significance between groups as determined by one-way ANOVA followed by Tukey HSD post hoc test. (B)–(G), Representative fluorescent images showing live (green) and dead (red) HaCaT cells submitted to H_2O_2 600 μM. (B) Cells treated with 0.4 μg/mL SHED-EVs. (C) Cells treated with 50% SHED-CM. (D) Cells treated with 0.4 μg/mL HaCaT-EVs (control). (E) Cells treated with 50% HaCaT-CM (control). (F) Cells treated with DMEM (control). (G) Cells without H_2O_2 pretreatment and treated only with DMEM. Scale bars = 277.5 μm.

reducing keratinocytes viability to 69% ± 7%. Previously HaCaT apoptosis models reported the use of 800 μM H_2O_2/4 h[49] or 1 mM H_2O_2/4 h.[50] However, these concentrations were lethal in the present experiments, necessitating the identification of an appropriate concentration and incubation time. Also, both SHED-CM and SHED-EVs demonstrated a mitigating effect on H_2O_2-induced apoptosis, indicating an active role of SHED secretome in wound healing. These findings align with the proteome profile obtained from SHED-CM, revealing an enrichment of stress-related proteins (164 proteins), as detailed in Table 1.

The potential of the secretome from various sources of stromal cells has been explored in both preclinical and clinical studies, demonstrating their therapeutic benefits in wound healing models. Specifically, the utilisation of exosomes derived from bone mesenchymal stem cells has been shown to accelerate wound closure, reduce scar formation, and enhance collagen deposition through the upregulation of miR-21-5p, in a full-thickness excisional wound model conducted in rats.[51] Also, exosomes isolated from adipose-derived stem cells (ASC) when administered intravenously, have demonstrated superiority over local injections by promoting early-stage collagen expression, consequently

leading to an accelerated wound-healing process in mice[52] and enhanced number of blood vessels in a full-thickness excisional wound model.[53] In the same way, exosomes isolated from ASC and from embryonic stem cells promoted higher vessel densities and accelerated wound healing in a pressure-induced ulcer model in aged mice.[54]

Exosomes derived from induced pluripotent stem cells accelerated wound healing, epithelization, and angiogenesis in a full-thickness excisional wound model in monkeys.[55] Additionally, exosomes isolated from umbilical cord-derived MSCs accelerated re-epithelialization in a model of second-degree burn injury in rats,[56] while those derived from urine-derived stem cell-induced higher amounts of blood vessels and collagen deposition in a full-thickness excisional wound model in diabetic mice.[57] While various studies have demonstrated a positive impact, it is well-established that the influence of exosomes on cellular biological processes is associated with both their source and the specific target cells. This suggests variations in the wound-healing potential of exosomes derived from MSCs originating from, for example, bone marrow, adipose tissue, or umbilical cord.[58]

In addition to exosomes, the conditioned medium has also been studied. A conditioned medium obtained from MSCs derived from amniotic fluid, which contains VEGF and TGF-β1, enhanced the growth and mobility of human dermal fibroblasts in vitro and promoted wound healing in vivo.[59] Still, the conditioned medium derived from bone marrow-derived MSCs reduced UV-induced MMP1 expression and maintained the synthesis of pro-collagen, contributing to the improvement of UV-induced skin damage in mice.[60]

Some clinical trials have also been carried out to evaluate the potential of therapies derived from stem/stromal cells to stimulate wound healing and the regeneration of skin tissues. Zhou et al. conducted studies on the effects of conditioned media collected from ASC following skin treatment with fractional carbon dioxide laser resurfacing.[61,62] The topical application of the conditioned medium was effective in enhancing wound healing by reducing transient adverse effects such as erythema, hyperpigmentation, and increased transepidermal water loss.[61] This therapy also resulted in heightened dermal collagen density and increased elastin density, effectively addressing atrophic acne scars and promoting skin rejuvenation.[62] In a randomised control trial, the use of a topical human amniotic membrane-mesenchymal stem cell-conditioned medium-vitamin E better-promoted wound healing in chronic plantar ulcers in leprosy.[63] Another clinical trial focused on atrophic post-acne scars revealed that dermal collagen was increased and the procollagen type I gene was upregulated when using topical stem cell-conditioned medium after a fractional carbon dioxide laser compared to only this laser.[64]

In a comparative study aimed at treating facial acne scars, the utilisation of exosomes derived from human ASC resulted in superior outcomes, including more positive responses, a quicker recovery period, and a reduced incidence of side effects.[65] Additionally, a randomised controlled study involving patients with aging skin who underwent ablative fractional laser treatment showed that the conditioned media from human ASC induced favourable effects. This

was likely achieved through the reduction of MMP-1 and MMP-2 expression and presented the enhancement of collagen 1 expression.[66]

Therefore, recent corroborations have suggested that the regenerative abilities of stem cell-based therapies may be influenced by secreted paracrine factors.

6 | CONCLUSION

In conclusion, our data demonstrate that SHED-CM and SHED-EVs enhance cell functions and increase VEGF expression in keratinocytes. SHEDs are an ideal source of CM and EVs for clinical applications because of their easy accessibility, excellent proliferation, and no associated morbidity. Both SHED-CM and SHED-EVs may be promising therapeutic tools for accelerating re-epithelialization in wound healing.

DATA AVAILABILITY STATEMENT
The data that support the findings of this study are available from the corresponding author upon reasonable request.

ORCID
Juliana Girón Bastidas https://orcid.org/0000-0003-3131-5067

REFERENCES

1. Liu H, Liu S, Qiu X, et al. Donor MSCs release apoptotic bodies to improve myocardial infarction via autophagy regulation in recipient cells. *Autophagy*. 2020;16(12):2140-2155. doi:10.1080/15548627.2020.1717128

2. Coppin L, Sokal E, Stéphenne X. Thrombogenic risk induced by intravascular mesenchymal stem cell therapy: current status and future perspectives. *Cell*. 2019;8(10):1-16. doi:10.3390/CELLS8101160

3. Janowski M, Lyczek A, Engels C, et al. Cell size and velocity of injection are major determinants of the safety of intracarotid stem cell transplantation. *J Cereb Blood Flow Metab*. 2013;33(6):921-927. doi:10.1038/jcbfm.2013.32

4. György B, Szabó TG, Pásztói M, et al. Membrane vesicles, current state-of-the-art: emerging role of extracellular vesicles. *Cell Mol Life Sci*. 2011;68(16):2667-2688. doi:10.1007/S00018-011-0689-3

5. Girón J, Maurmann N, Pranke P. The role of stem cell-derived exosomes in the repair of cutaneous and bone tissue. *J Cell Biochem*. 2021;123:183-201. doi:10.1002/JCB.30144

6. Miura M, Gronthos S, Zhao M, et al. SHED: stem cells from human exfoliated deciduous teeth. *Proc Natl Acad Sci USA*. 2003;100(10):5807-5812. doi:10.1073/PNAS.0937635100

7. Casagrande L, Cordeiro MM, Nör SA, Nör JE. Dental pulp stem cells in regenerative dentistry. *Odontology*. 2011;99(1):1-7. doi:10.1007/S10266-010-0154-Z

8. Matsushita Y, Ishigami M, Matsubara K, et al. Multifaceted therapeutic benefits of factors derived from stem cells from human exfoliated deciduous teeth for acute liver failure in rats. *J Tissue Eng Regen Med*. 2017;11(6):1888-1896. doi:10.1002/TERM.2086

9. Yamagata M, Yamamoto A, Kako E, et al. Human dental pulp-derived stem cells protect against hypoxic-ischemic brain injury in neonatal mice. *Stroke*. 2013;44(2):551-554. doi:10.1161/STROKEAHA.112.676759

10. Tsuruta T, Sakai K, Watanabe J, Katagiri W, Hibi H. Dental pulp-derived stem cell conditioned medium to regenerate peripheral nerves in a novel animal model of dysphagia. *PLoS One*. 2018;13(12):e0208938. doi:10.1371/JOURNAL.PONE.0208938

11. Chen YR, Lai PL, Chien Y, et al. Improvement of impaired motor functions by human dental exfoliated deciduous teeth stem cell-derived factors in a rat model of Parkinson's disease. *Int J Mol Sci*. 2020;21(11):3807. doi:10.3390/IJMS21113807

12. Mita T, Furukawa-Hibi Y, Takeuchi H, et al. Conditioned medium from the stem cells of human dental pulp improves cognitive function in a mouse model of Alzheimer's disease. *Behav Brain Res*. 2015;293:189-197. doi:10.1016/J.BBR.2015.07.043

13. Shimojima C, Takeuchi H, Jin S, et al. Conditioned medium from the stem cells of human exfoliated deciduous teeth ameliorates experimental autoimmune encephalomyelitis. *J Immunol*. 2016;196(10):4164-4171. doi:10.4049/JIMMUNOL.1501457

14. Miura-Yura E, Tsunekawa S, Naruse K, et al. Secreted factors from cultured dental pulp stem cells promoted neurite outgrowth of dorsal root ganglion neurons and ameliorated neural functions in streptozotocin-induced diabetic mice. *J Diabetes Investig*. 2020;11(1):28-38. doi:10.1111/JDI.13085

15. Inoue T, Sugiyama M, Hattori H, Wakita H, Wakabayashi T, Ueda M. Stem cells from human exfoliated deciduous tooth-derived conditioned medium enhance recovery of focal cerebral ischemia in rats. *Tissue Eng Part A*. 2013;19(1–2):24-29. doi:10.1089/TEN.TEA.2011.0385

16. Asadi-Golshan R, Razban V, Mirzaei E, et al. Efficacy of dental pulp-derived stem cells conditioned medium loaded in collagen hydrogel in spinal cord injury in rats: stereological evidence. *J Chem Neuroanat*. 2021;116:101978. doi:10.1016/J.JCHEMNEU.2021.101978

17. Li XX, Yuan X-J, Zhai Y, et al. Treatment with stem cells from human exfoliated deciduous teeth and their derived conditioned medium improves retinal visual function and delays the degeneration of photoreceptors. *Stem Cells Dev*. 2019;28(22):1514-1526. doi:10.1089/SCD.2019.0158

18. Pivoraitė U, Jarmalavičiūtė A, Tunaitis V, et al. Exosomes from human dental pulp stem cells suppress carrageenan-induced acute inflammation in mice. *Inflammation*. 2015;38(5):1933-1941. doi:10.1007/S10753-015-0173-6

19. Yamaguchi S, Shibata R, Yamamoto N, et al. Dental pulp-derived stem cell conditioned medium reduces cardiac injury following ischemia-reperfusion. *Sci Rep*. 2015;5:1-10. doi:10.1038/SREP16295

20. Gunawardena TNA, Masoudian Z, Rahman MT, Ramasamy TS, Ramanathan A, Kasim NHA. Dental derived stem cell conditioned media for hair growth stimulation. *PLoS One*. 2019;14(5):e0216003. doi:10.1371/JOURNAL.PONE.0216003

21. de Cara SPHM, Origassa CST, de Sá Silva F, et al. Angiogenic properties of dental pulp stem cells conditioned medium on endothelial cells in vitro and in rodent orthotopic dental pulp regeneration. *Heliyon*. 2019;5(4):e01560. doi:10.1016/J.HELIYON.2019.E01560

22. Hiraki T, Kunimatsu R, Nakajima K, et al. Stem cell-derived conditioned media from human exfoliated deciduous teeth promote bone regeneration. *Oral Dis*. 2020;26(2):381-390. doi:10.1111/ODI.13244

23. Wei J, Song Y, du Z, et al. Exosomes derived from human exfoliated deciduous teeth ameliorate adult bone loss in mice through promoting osteogenesis. *J Mol Histol*. 2020;51(4):455-466. doi:10.1007/S10735-020-09896-3

24. Ishikawa J, Takahashi N, Matsumoto T, et al. Factors secreted from dental pulp stem cells show multifaceted benefits for treating experimental rheumatoid arthritis. *Bone*. 2016;83:210-219. doi:10.1016/J.BONE.2015.11.012

25. Ogasawara N, Kano F, Hashimoto N, et al. Factors secreted from dental pulp stem cells show multifaceted benefits for treating experimental temporomandibular joint osteoarthritis. *Osteoarthr Cartil*. 2020;28(6):831-841. doi:10.1016/J.JOCA.2020.03.010

26. Izumoto-Akita T, Tsunekawa S, Yamamoto A, et al. Secreted factors from dental pulp stem cells improve glucose intolerance in streptozotocin-induced diabetic mice by increasing pancreatic β-cell function. *BMJ Open Diabetes Res Care*. 2015;3(1):e000128. doi:10.1136/BMJDRC-2015-000128

27. Wakayama H, Hashimoto N, Matsushita Y, et al. Factors secreted from dental pulp stem cells show multifaceted benefits for treating acute lung injury in mice. *Cytotherapy*. 2015;17(8):1119-1129. doi:10.1016/J.JCYT.2015.04.009

28. Xie Y, Yu L, Cheng Z, et al. SHED-derived exosomes promote LPS-induced wound healing with less itching by stimulating macrophage autophagy. *J Nanobiotechnol*. 2022;20(1):1-21. doi:10.1186/S12951-022-01446-1

29. de S. P. A. Dos Santos FP, Peruch T, Katami SJV, et al. Poly (lactide-co-glycolide) (PLGA) scaffold induces short-term nerve regeneration and functional recovery following sciatic nerve transection in rats. *Neuroscience*. 2019;396:94-107. doi:10.1016/J.NEUROSCIENCE.2018.11.007

30. Bernardi L, Luisi SB, Fernandes R, et al. The isolation of stem cells from human deciduous teeth pulp is related to the physiological process of resorption. *J Endod*. 2011;37(7):973-979. doi:10.1016/J.JOEN.2011.04.010

31. Raudvere U, Kolberg L, Kuzmin I, et al. G:profiler: a web server for functional enrichment analysis and conversions of gene lists (2019 update). *Nucleic Acids Res*. 2019;47(W1):W191-W198. doi:10.1093/NAR/GKZ369

32. Smith PK, Krohn RI, Hermanson GT, et al. Measurement of protein using bicinchoninic acid. *Anal Biochem*. 1985;150(1):76-85. doi:10.1016/0003-2697(85)90442-7

33. Suárez H, Gámez-Valero A, Reyes R, et al. A bead-assisted flow cytometry method for the semi-quantitative analysis of extracellular vesicles. *Sci Rep*. 2017;7(1):1-11. doi:10.1038/s41598-017-11249-2

34. Schmittgen, T., Livak, K. "Analyzing real-time PCR data by the comparative CT method." *Nat Protoc 3*, 1101–1108. 2008. https://doi.org/10.1038/nprot.2008.73

35. Dabrowska S, Andrzejewska A, Janowski M, Lukomska B. Immunomodulatory and regenerative effects of mesenchymal stem cells and extracellular vesicles: therapeutic outlook for inflammatory and degenerative diseases. *Front Immunol*. 2020;11:1-26. doi:10.3389/FIMMU.2020.591065

36. Pastar I, Stojadinovic O, Yin NC, et al. Epithelialization in wound healing: A comprehensive review. *Adv Wound Care*. 2014;3(7):445-464. doi:10.1089/WOUND.2013.0473

37. Rousselle P, Braye F, Dayan G. Re-epithelialization of adult skin wounds: cellular mechanisms and therapeutic strategies. *Adv Drug Deliv Rev*. 2019;146:344-365. doi:10.1016/J.ADDR.2018.06.019

38. Aragona M, Dekoninck S, Rulands S, et al. Defining stem cell dynamics and migration during wound healing in mouse skin epidermis. *Nat Commun*. 2017;8(1):1468. doi:10.1038/ncomms14684

39. Sugawara T, Gallucci RM, Simeonova PP, Luster MI. Regulation and role of interleukin 6 in wounded human epithelial keratinocytes. *Cytokine*. 2001;15(6):328-336. doi:10.1006/CYTO.2001.0946

40. Choi JH, Jun JH, Kim JH, Sung HJ, Lee JH. Synergistic effect of interleukin-6 and hyaluronic acid on cell migration and ERK activation in human keratinocytes. *J Korean Med Sci*. 2014;29(Suppl 3):S210-S216. doi:10.3346/JKMS.2014.29.S3.S210

41. Yoshizaki K, Nishimoto N, Matsumoto K, et al. Interleukin 6 and expression of its receptor on epidermal keratinocytes. *Cytokine*. 1990;2(5):381-387. doi:10.1016/1043-4666(90)90069-6

42. Kroeze KL, Boink MA, Sampat-Sardjoepersad SC, Waaijman T, Scheper RJ, Gibbs S. Autocrine regulation of re-epithelialization after wounding by chemokine receptors CCR1, CCR10, CXCR1, CXCR2, and CXCR3. *J Invest Dermatol*. 2012;132(1):216-225. doi:10.1038/JID.2011.245

43. Rennekampff HO, Hansbrough JF, Kiessig V, Doré C, Sticherling M, Schröder JM. Bioactive interleukin-8 is expressed in wounds and enhances wound healing. *J Surg Res*. 2000;93(1):41-54. doi:10.1006/jsre.2000.5892

44. Brown LF, Yeo KT, Berse B, et al. Expression of vascular permeability factor (vascular endothelial growth factor) by epidermal keratinocytes during wound healing. *J Exp Med*. 1992;176(5):1375-1379. doi:10.1084/JEM.176.5.1375

45. Man XY, Yang XH, Cai SQ, Yao YG, Zheng M. Immunolocalization and expression of vascular endothelial growth factor receptors (VEGFRs) and neuropilins (NRPs) on keratinocytes in human epidermis. *Mol Med*. 2006;12(7–8):127-136. doi:10.2119/2006-00024.MAN/FIGURES/6

46. Wilgus TA, Matthies AM, Radek KA, et al. Novel function for vascular endothelial growth factor Receptor-1 on epidermal keratinocytes. *Am J Pathol*. 2005;167(5):1257-1266. doi:10.1016/S0002-9440(10)61213-8

47. Bhandi S, al Khatani A, Abdulaziz Sumayli H, et al. Comparative analysis of cytokines and growth factors in the conditioned media of stem cells from the pulp of deciduous, young, and old permanent tooth. *Saudi J Biol Sci*. 2021;28(6):3559-3565. doi:10.1016/J.SJBS.2021.03.031

48. Kang CM, Shin MK, Jeon M, Lee YH, Song JS, Lee JH. Distinctive cytokine profiles of stem cells from human exfoliated deciduous teeth and dental pulp stem cells. *J Dent Sci*. 2022;17(1):276-283. doi:10.1016/J.JDS.2021.03.019

49. Ma T, Fu B, Yang X, Xiao Y, Pan M. Adipose mesenchymal stem cell-derived exosomes promote cell proliferation, migration, and inhibit cell apoptosis via Wnt/β-catenin signaling in cutaneous wound healing. *J Cell Biochem*. 2019;120(6):10847-10854. doi:10.1002/JCB.28376

50. Zhao G, Liu F, Liu Z, et al. MSC-derived exosomes attenuate cell death through suppressing AIF nucleus translocation and enhance cutaneous wound healing. *Stem Cell Res Ther*. 2020;11(1):174. doi:10.1186/S13287-020-01616-8

51. Wu D, Kang L, Tian J, et al. Exosomes derived from bone mesenchymal stem cells with the stimulation of Fe3O4 nanoparticles and static magnetic field enhance wound healing through upregulated miR-21-5p. *Int J Nanomedicine*. 2020;15:7979-7993. doi:10.2147/IJN.S27565

52. Hu L, Wang J, Zhou X, et al. Exosomes derived from human adipose mensenchymal stem cells accelerates cutaneous wound healing via optimizing the characteristics of fibroblasts. *Sci Rep*. 2016;6:32993. doi:10.1038/srep32993

53. Zhang W, Bai X, Zhao B, et al. Cell-free therapy based on adipose tissue stem cell-derived exosomes promotes wound healing via the PI3K/Akt signaling pathway. *Exp Cell Res*. 2018;370(2):333-342. doi:10.1016/j.yexcr.2018.06.035

54. Chen B, Sun Y, Zhang J, et al. Human embryonic stem cell-derived exosomes promote pressure ulcer healing in aged mice by rejuvenating senescent endothelial cells. *Stem Cell Res Ther*. 2019;10(1):142. doi:10.1186/s13287-019-1253-6

55. Lu M, Peng L, Ming X, et al. Enhanced wound healing promotion by immune response-free monkey autologous iPSCs and exosomes vs. their allogeneic counterparts. *EBioMedicine*. 2019;42:443-457. doi:10.1016/j.ebiom.2019.03.011

56. Zhang B, Wu X, Zhang X, et al. Human umbilical cord mesenchymal stem cell exosomes enhance angiogenesis through the Wnt4/β-catenin pathway. *Stem Cells Transl Med*. 2015;4(5):513-522. doi:10.5966/sctm.2014-0267

57. Chen CY, Rao SS, Ren L, et al. Exosomal DMBT1 from human urine-derived stem cells facilitates diabetic wound repair by promoting angiogenesis. *Theranostics*. 2018;8(6):1607-1623. doi:10.7150/thno.22958

58. Hoang DH, Nguyen TD, Nguyen HP, et al. Differential wound healing capacity of mesenchymal stem cell-derived exosomes originated from bone marrow, adipose tissue and umbilical cord under serum-and xeno-free condition. *Front Mol Biosci*. 2020;7:119. doi:10.3389/fmolb.2020.00119

59. Jun EK, Zhang Q, Yoon B, et al. Hypoxic conditioned medium from human amniotic fluid-derived mesenchymal stem cells accelerates skin wound healing through TGF-β/SMAD2 and PI3K/Akt pathways. *Int J Mol Sci*. 2014;15(1):605-628. doi:10.3390/ijms15010605

60. Kwon TR, Oh CT, Choi EJ, et al. Conditioned medium from human bone marrow-derived mesenchymal stem cells promotes skin moisturization and effacement of wrinkles in UVB-irradiated SKH-1 hairless mice. *Photodermatol Photoimmunol Photomed*. 2016;32(3):120-128. doi:10.1111/phpp.12224

61. Zhou BR, Xu Y, Guo SL, et al. The effect of conditioned media of adipose-derived stem cells on wound healing after ablative fractional carbon dioxide laser resurfacing. *Biomed Res Int*. 2013;2013:519126. doi:10.1155/2013/519126

62. Zhou BR, Zhang T, Bin Jameel AA, et al. The efficacy of conditioned media of adipose-derived stem cells combined with ablative carbon dioxide fractional resurfacing for atrophic acne scars and skin rejuvenation. *J Cosmet Laser Ther*. 2016;18(3):138-148. doi:10.3109/14764172.2015.1114638

63. Prakoeswa CS, Natallya F, Harnindya D, et al. The efficacy of topical human amniotic membrane-mesenchymal stem cell-conditioned medium (hAMMSC-CM) and a mixture of topical hAMMSC-CM+ vitamin C and hAMMSC-CM+ vitamin E on chronic plantar ulcers in leprosy: a randomized control trial. *J Dermatol Treat*. 2018;29(8):835-840.

64. Abdel-Maguid EM, Awad SM, Hassan YS, el-Mokhtar MA, el-Deek HEM, Mekkawy MMA. Efficacy of stem cell-conditioned medium vs. platelet-rich plasma as an adjuvant to ablative fractional CO_2 laser resurfacing for atrophic post-acne scars: a split-face clinical trial. *J Dermatol Treat*. 2021;32(2):242-249. doi:10.1080/09546634.2019.1630701

65. Kwon HH, Yang SH, Lee J, et al. Combination treatment with human adipose tissue stem cell-derived exosomes and fractional CO_2 laser for acne scars: A 12-week prospective, double-blind, randomized, Split-face study. *Acta Derm Venereol*. 2020;100(18):adv00310. doi:10.2340/00015555-3666

66. Lee YI, Kim S, Kim J, Kim J, Chung KB. Randomized controlled study for the anti-aging effect of human adipocyte-derived mesenchymal stem cell media combined with niacinamide after laser therapy. *J Cosmet Dermatol*. 2021;20:1774-1781. doi:10.1111/jocd.13767

SUPPORTING INFORMATION

Additional supporting information can be found online in the Supporting Information section at the end of this article.